

Cryogenic mechanical loss of a single-crystalline GaP coating layer for precision measurement applications

Peter G. Murray,^{*} Iain W. Martin,[†] Kieran Craig, James Hough, and Sheila Rowan
SUPA, School of Physics and Astronomy, University of Glasgow, Glasgow, G12 8QQ, Scotland

Riccardo Bassiri, Martin M. Fejer, James S. Harris, Brian T. Lantz,
 Angie C. Lin, Ashot S. Markosyan, and Roger K. Route
Edward L Ginzton Laboratory, Stanford University, Stanford, California 94304, USA
 (Received 16 November 2016; published 17 February 2017)

The first direct observations of gravitational waves have been made by the Advanced LIGO detectors. However, the quest to improve the sensitivities of these detectors remains, and epitaxially grown single-crystal coatings show considerable promise as alternatives to the ion-beam sputtered amorphous mirror coatings typically used in these detectors and other such precision optical measurements. The mechanical loss of a 1 μm thick single-crystalline gallium phosphide (GaP) coating, incorporating a buffer layer region necessary for the growth of high quality epitaxial coatings, has been investigated over a broad range of frequencies and with fine temperature resolution. It is shown that at 20 K the mechanical loss of GaP is a factor of 40 less than an undoped tantala film heat-treated to 600 °C and is comparable to the loss of a multilayer GaP/AlGaP coating. This is shown to translate into possible reductions in coating thermal noise of a factor of 2 at 120 K and 5 at 20 K over the current best IBS coatings (alternating stacks of silica and titania-doped tantala). There is also evidence of a thermally activated dissipation process between 50 and 70 K.

DOI: [10.1103/PhysRevD.95.042004](https://doi.org/10.1103/PhysRevD.95.042004)

I. INTRODUCTION

Future long-baseline interferometric gravitational wave detectors are proposed with operation at cryogenic temperatures [1–5]. These detectors will be used in the observation of gravitational radiation emitted from a range of astrophysical bodies [6]. The first such direct detections have already been announced by the LIGO Collaboration using the Advanced LIGO gravitational wave detectors [7,8]. Assuming appropriate choices for mirror and suspension materials, cooling these detector parts should result in thermal-noise limited sensitivities considerably below those of current detectors [9–13]. The current generation of detectors is designed in such a way that a passing gravitational wave will induce a displacement of highly reflective mirrors suspended as pendulums at the end of each of the two interferometer arms [9]. In the case of gravitational wave astronomy it is expected that one significant limit to the sensitivity of the detectors is set by thermal noise associated with the mirror coatings applied to the test masses to reflect the 1064 nm laser light used to illuminate the interferometers [10,14–17]. Coating thermal

noise is also expected to limit the performance of other cases of precision interferometry as is commonly used in several areas of fundamental and applied science, for example, in the cavities of high-precision frequency-stabilized lasers [18–20], in high-resolution optical spectroscopy [21], in optical frequency standards [22] and in fundamental quantum measurements [23].

The use of cryogenic cooling to reduce the temperature to either 20 K or 120 K has been suggested as part of the long-term upgrade strategy to improve the detector sensitivity of the Advanced LIGO detectors [2,3], while the proposed Einstein Telescope low frequency detector would operate at 10 K [24–27]. Operation at low temperature will require a change of the test-mass material, since the mechanical loss, and therefore the thermal noise, of fused silica increases rapidly at low temperature, with a broad loss peak at approximately 40 K [28–31]. Crystalline silicon has been proposed as an alternative test-mass substrate due to its low mechanical loss at cryogenic temperatures [32] and its favorable thermal properties [33–35]. However, silicon is not transparent at 1064 nm and thus the use of silicon optics would require a change in the interferometer laser wavelength, with wavelengths around 1550–2000 nm currently under consideration [36,37].

Single-crystalline coating materials, grown using molecular beam epitaxy (MBE), are an exciting possible alternative to amorphous ion-beam sputtered coatings for use in an interferometric detector operating at 1550 nm. Cole *et al.* [38] reported mechanical losses of 2.5×10^{-5} at

^{*}peter.murray@glasgow.ac.uk
[†]iain.martin@glasgow.ac.uk

Published by the American Physical Society under the terms of the Creative Commons Attribution 4.0 International license. Further distribution of this work must maintain attribution to the author(s) and the published article's title, journal citation, and DOI.

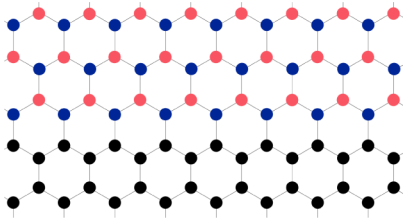


FIG. 1. Schematic cross section of an ideal defect-free GaP (alternating red and blue dots) on Si (black dots) interface where there is a uniform monolayer of either all Ga or all P atoms along the Si surface.

room temperature for freestanding multilayer gallium arsenide/aluminium gallium arsenide (GaAs/AlGaAs) microfabricated mechanical resonators; a factor of approximately 10 lower than an equivalent ion-beam sputtered silica/tantala coating. The lattice constants of GaAs and AlAs are 5.6533 Å and 5.6611 Å, respectively, whereas the lattice constant of silicon is lower 5.4310 Å [39,40]. As a consequence, GaAs/AlGaAs coatings are not able to be grown directly on silicon mirror substrates and instead have to be grown on GaAs substrates and then transferred, and bonded, onto the final mirror substrate [38].

A promising alternative crystalline coating is multilayers of gallium phosphide (GaP) and aluminium gallium phosphide (AlGaP) due to the minimal lattice mismatch between these materials and silicon. The lattice constants of GaP and AlP are 5.4505 Å and 5.4510 Å, respectively, allowing these materials and their alloys to be successfully epitaxially grown directly onto silicon [41,42]. Recent measurements of a GaP/AlGaP multilayer coating found mechanical losses of $1.4\text{--}3.7 \times 10^{-5}$ at 12 K, similar to those reported for GaAs/AlGaAs [43].

Growing high quality III-V epitaxial films on silicon substrates, as represented in Fig. 1, free from cracks and high density dislocations is challenging. Cracks can be induced due to residual stress in the films from any mismatch between the crystal lattices of the III-V layer and the silicon substrate and from their differing thermal expansion coefficients. A buffer layer, typically a few hundred nanometers thick, is often grown between the substrate and the desired epitaxial structure to eradicate any remaining lattice mismatch and to suppress the formation of antiphase domains, an example of which is shown in Fig. 2 [44]. The quality of any MBE grown III-V multilayer coating depends strongly on the effectiveness of this underlying buffer layer. In the case of a gallium phosphide (GaP) buffer layer, these antiphase defects arise from the bonding of phosphorous-to-phosphorous or gallium-to-gallium, resulting in a region in the crystal coating where the atoms are configured in the opposite order to those in an ideal lattice.

These antiphase domains are found more commonly at the interface with the parent lattice and are eradicated by ensuring that the surface of the silicon substrate has double

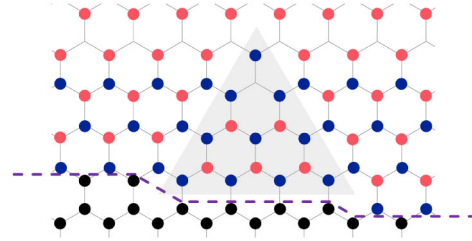


FIG. 2. Schematic cross section of an example of an antiphase defect region created by a step (dashed line) on the Si surface (black dots). The shaded region highlights two antiphase boundaries, where the atoms are configured with Ga-to-Ga or P-to-P bonding (here blue-to-blue), which self-annihilate.

atomic steps [44]. Once the GaP buffer layer has been deposited on the silicon substrate, the desired epitaxial structure can be grown. Here mechanical loss measurements of a 1 μm thick GaP layer grown using molecular beam epitaxy on a silicon substrate are presented to investigate the mechanical loss of the first layer of GaP grown on a silicon substrate.

II. SAMPLE PREPARATION

The 1 μm thick gallium phosphide coating was grown on a silicon wafer using MBE. The coating was grown onto a 3" diameter Si wafer, off-cut by 4 deg towards the [110]

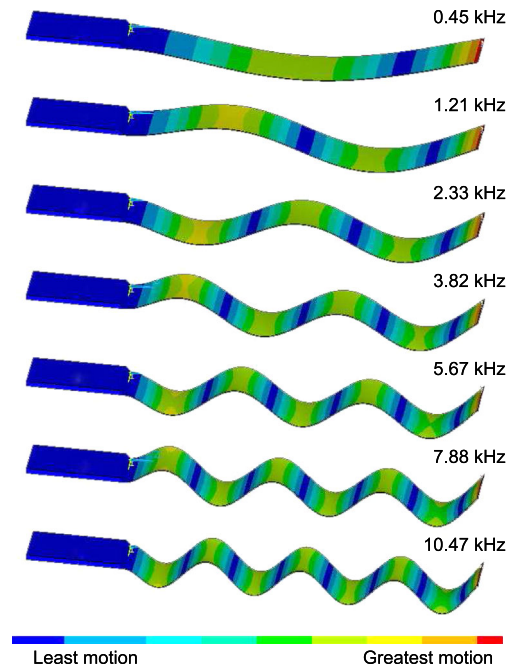


FIG. 3. Finite element analysis representation of the 0.45 kHz, 1.21 kHz, 2.33 kHz, 3.82 kHz, 5.67 kHz, 7.88 kHz and 10.47 kHz bending modes of the silicon cantilever. The cantilever length is parallel to the [110] crystal axis. The coating is grown onto the underside of the flexure. The 7.88 kHz bending mode was observed to strongly couple with a torsional resonant mode of a similar frequency.

axis. Cantilever structures, each consisting of a 0.5 mm “clamping block” and longer vibrating section 45 mm long by 5 mm wide and $55.7 \mu\text{m}$ in thickness, were fabricated from the coated wafer using reactive ion etching. The cantilever structures were designed to be comparable with the cantilevers used in the investigations of amorphous coatings [45–47]. The shape of the cantilever can be seen in the finite element representation of the shapes of the bending modes in Fig. 3.

The coating was grown on the silicon substrate by MBE using a two-step growth process of nucleation of atoms on the surface and ordered overgrowth, enabling the decoupling of the formation and growth of antiphase domains [44]. The growth was carried out with a low V/III flux ratio and low growth rate to maximize the annihilation of antiphase domains in the GaP layer [44]. This constrains any antiphase domains to the first ~ 30 nm of the buffer layer allowing the overgrowth of the GaP material to be defect free [44]. *In situ* reflection high-energy electron diffraction was used to measure the growth of the layer until it was determined to be $1 \mu\text{m}$ thick [48].

III. EXPERIMENTAL PROCEDURE

A temperature dependent upper limit of the mechanical loss of the $1 \mu\text{m}$ thick GaP coating, $\phi(\omega_0)_{\text{GaP}}$, was estimated by measuring the mechanical loss of the bending resonant modes of the cantilever coated with GaP at a range of temperatures and comparing it with the expected loss of a similar uncoated silicon substrate [49],

$$\phi(\omega_0)_{\text{GaP}} = \frac{Y_{\text{Si}} t_{\text{Si}}}{3Y_{\text{GaP}} t_{\text{GaP}}} (\phi(\omega_0)_{\text{Si \& GaP}} - \phi(\omega_0)_{\text{Si}}). \quad (1)$$

where ω_0 is the angular frequency of the bending mode, $\phi(\omega_0)_{\text{Si \& GaP}}$ is the measured loss factor of the silicon cantilever with a GaP buffer layer and $\phi(\omega_0)_{\text{Si}}$ is the loss factor of the silicon substrate. Here, the uncoated loss was taken to be the expected level of thermoelastic loss of a $55.7 \mu\text{m}$ thick silicon cantilever from Zener *et al.* to provide an upper limit to the coating loss [50,51]. t_{Si} and Y_{Si} are the thickness and Young’s modulus of the silicon substrate respectively and t_{GaP} and Y_{GaP} are the thickness and Young’s modulus of the GaP layer. The Young’s modulus of silicon and gallium phosphide were taken to be 166 GPa [52] and 103 GPa [41,53].

The cantilever was securely mounted to the liquid helium cooled baseplate of a temperature-controlled cryostat [54]. Measurements were carried out under vacuum ($< 10^{-6}$ mbar) to prevent any gas damping effects. The bending modes of the sample were excited in turn using an electrostatic actuator positioned a few millimeters below the cantilever. Figure 3 shows ANSYS® finite element analysis models of the second to eighth order bending modes of the silicon cantilever. The dissipation of these bending modes $\phi(\omega_0)$ can then be found from a fit to the free exponential decay of the resonant motion [49]

$$A(t) = A_0 e^{-\phi(\omega_0)\omega_0 t/2}. \quad (2)$$

The motion was sensed by illuminating the oscillating end of the cantilever with a laser beam and monitoring the resulting shadow with a split photodiode sensor. In each measurement cycle the temperature of the cantilever was increased systematically from approximately 10 K to 300 K, maintained typically to within 0.1 K of the set-point using a PID controller, and completely re-clamped between cycles. The temperature of the cantilever was recorded using a silicon-diode sensor mounted inside a small hole on the stainless steel clamp situated close to the thick end of the flexure. This loss measuring technique is discussed in greater detail by Martin *et al.* [45].

IV. RESULTS AND ANALYSIS

Figure 4 shows the measured mechanical loss obtained for the silicon cantilever coated with $1 \mu\text{m}$ of GaP for the resonant modes at approximately 0.45 kHz, 1.21 kHz, 2.33 kHz, 3.82 kHz, 5.67 kHz and 10.47 kHz. The data from the 7.88 kHz bending mode is not included because it was observed to be strongly coupled with a torsional resonant mode of a similar frequency making it difficult to obtain a clean exponential ring-down measurement.

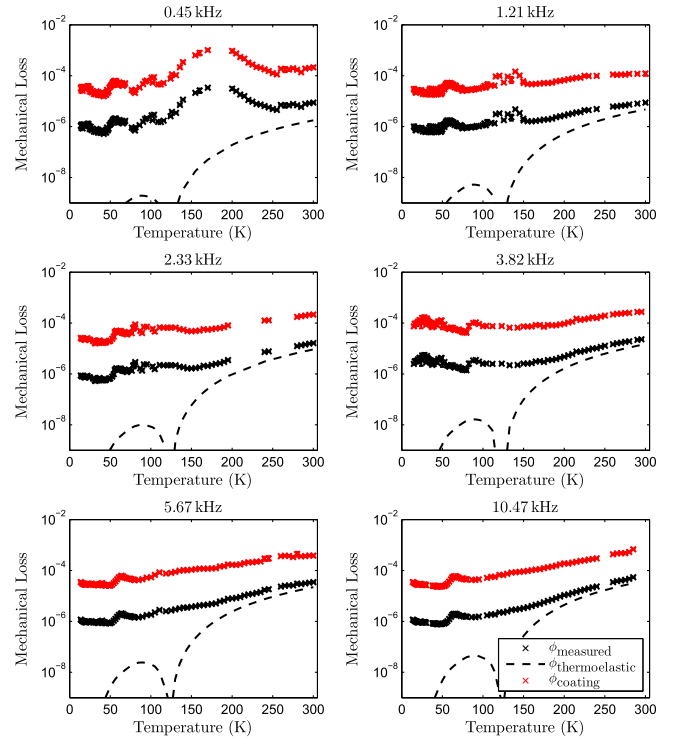


FIG. 4. Upper limit for the GaP coating mechanical loss of the 0.45 kHz, 1.21 kHz, 2.33 kHz, 3.82 kHz, 5.67 kHz and 10.47 kHz bending modes (red) calculated from the measured mechanical loss of the GaP coated cantilever (black) at these frequencies. The dashed line shows the expected level of thermoelastic loss of the silicon cantilever substrate at these frequencies.

These measured mechanical losses were compared with the calculated levels of thermoelastic loss of the $55.7 \mu\text{m}$ thick silicon substrate at each of the resonant frequencies and the upper limit of the mechanical loss of the GaP layer was calculated using Eq. (1). Figure 4 indicates that the loss decreases generally with temperature.

At 295 K the average loss of the GaP layer was $3.5 \pm 0.8 \times 10^{-4}$, which is approximately 2 orders of magnitude higher than the loss reported in epitaxially grown GaP microdisks by Mitchell *et al.* [55]. It is however, comparable to the 3×10^{-4} reported loss of tantala and 2.4×10^{-4} loss of titania-doped tantala at this temperature [46]. The microdisk studied by Mitchell *et al.* [55] was grown on a gallium phosphide substrate whereas the GaP film investigated here was grown directly onto silicon, so the higher room temperature mechanical loss here is likely to be a result of defect driven process associated with the epitaxial growth on silicon.

The loss of the 3.82 kHz resonant mode studied here shows some scatter below 70 K, possibly due to coupling with a torsional mode at a nearby frequency, but the average loss at 20 K of the other five resonant modes was found to be $2.7 \pm 0.2 \times 10^{-5}$, which is comparable to the losses measured on a GaP/AlGaP multilayer stack grown using MBE on a silicon disc [43]. This also suggests the loss of GaP is either equal to or greater than the loss of AlGaP. The peak in the 0.45 kHz resonant mode at 180 K and in the 1.21 kHz mode at 120 K were not observed for any of the higher order modes and are likely to be related to either coupling with a torsional mode at those temperatures or to energy loss into the clamp. There is evidence of a loss peak in every mode, observed between 50 and 70 K.

Table I summarizes the average loss of the GaP coating at a selection of temperatures, near to which a future interferometric gravitational wave detector may operate [1,2], for comparison with the coating loss of an undoped tantala film heat-treated to 600 °C [45]. At 14 K, the lowest temperature possible for comparison, the loss of the GaP coating was found to be a factor of 23 less than the tantala film. In tantala there is a peak in the loss that is not present in GaP and as a consequence the loss of the GaP coating is observed to be a factor of 40 lower at 20 K. Excluding the 1.21 kHz mode, at 120 K the average loss of GaP was found to be a factor of 7 lower than tantala.

TABLE I. Average loss of GaP at 14 K, 20 K and 120 K compared with the coating loss of an undoped tantala film heat-treated to 600 °C [45].

| Coating | Average coating mechanical loss ($\times 10^{-4}$) | | |
|--------------------------------|--|-----------------|-----------------|
| | 14 K | 20 K | 120 K |
| GaP | 0.39 ± 0.08 | 0.27 ± 0.02 | 0.77 ± 0.07 |
| Ta ₂ O ₅ | 9.0 ± 1.0 | 10.7 ± 1.3 | 5.2 ± 0.3 |

Cumming *et al.* observed that there were some small visible defects on the multilayer GaP/AlGaP crystalline coating whose losses are reported in [43], and noted that these degraded as the sample was temperature-cycled to cryogenic temperatures. However, there was no evidence, for the coatings studied here, of any damage following the temperature cycling of the single layer $1 \mu\text{m}$ thick GaP coating.

V. ARRHENIUS ANALYSIS OF LOSS PEAKS IN GAP FILM

A peak in the loss of the GaP layer was observed between 50 and 70 K (as shown in Fig. 4), with the temperature of the peak increasing with frequency. Further possible indications of this peak are visible in Cumming *et al.* where the coating loss of a GaP/AlGaP multilayer coating was observed to begin increasing above 40 K [43]. This behavior is characteristic of a thermally activated dissipation process. Such processes can be characterized by a rate constant, τ_0 , and an activation energy, E_a , which are related by the Arrhenius equation [56],

$$\tau = \tau_0 \exp\left(\frac{E_a}{k_B T}\right) \quad (3)$$

where τ is the relaxation time associated with the dissipative system returning to its equilibrium after being perturbed. The temperature of the dissipation peak T_{peak} , at resonant angular frequency ω_0 , is related to the activation energy and rate constant using the following [56]:

$$\omega_0 \tau_0 \exp\left(\frac{E_a}{k_B T_{\text{peak}}}\right) = 1. \quad (4)$$

Therefore, plotting $\log \omega_0$ against $1/T_{\text{peak}}$ should give a straight line fit, from which the activation energy and rate constant for the dissipation process can be calculated. Figure 5 shows this analysis for the peak in the mechanical

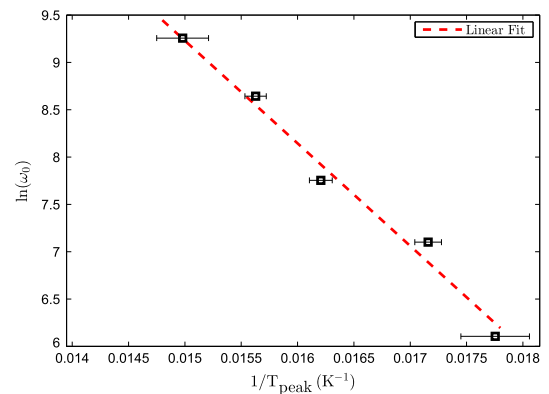


FIG. 5. Arrhenius plot of the loss peaks at 50–70 K observed in the GaP coating layer.

loss, observed between 50 and 70 K, of the GaP layer. The activation energy and rate constant calculated from this linear fit, were found to be (94.7 ± 7.0) meV and $(6.7 \pm 0.3) \times 10^{-12}$ s respectively. The exact origin of this loss peak is not known, but it could be attributed to either impurity defects in the crystal structure of the $1 \mu\text{m}$ thick gallium phosphide coating or to defects within the buffer layer.

VI. ESTIMATION OF THE THERMAL NOISE OF A MULTILAYER GaP/AlGaP FILM

Using the mechanical loss presented here for a single layer of GaP, known to be similar to a multilayer MBE GaP/AlGaP coating, the thermal noise performance of a GaP/AlGaP mirror coating at low temperature can be estimated. In order to achieve the same optical reflectivity as a current Advanced LIGO End Test Mass (ETM) coating (99.99995%), a total of 116 alternating layers of $\lambda/4$ optical thickness (here, $\lambda = 1550$ nm) GaP and AlGaP would be required, resulting in a total coating thickness of $15.5 \mu\text{m}$ [43] which is a factor of 1.8 thicker than an Advanced LIGO ETM coating on a silicon substrate correspondingly adjusted to function at 1550 nm.

The power spectral density of coating thermal noise can be approximated as [16],

$$S_x(f) = \frac{2k_B T}{\sqrt{\pi^3} f} \frac{1 - \sigma^2}{w_0 Y} \left\{ \phi_{\text{substrate}} + \frac{1}{\sqrt{\pi} w_0} \frac{d}{Y Y' (1 - \sigma'^2)(1 - \sigma^2)} \times [Y'^2 (1 + \sigma)^2 (1 - 2\sigma)^2 \phi_{\parallel} + Y Y' \sigma' (1 + \sigma)(1 + \sigma')(1 - 2\sigma)(\phi_{\parallel} - \phi_{\perp}) + Y^2 (1 + \sigma')^2 (1 - 2\sigma') \phi_{\perp}] \right\}, \quad (5)$$

where f is frequency in Hz, T is temperature in Kelvin, Y and σ are the Young's modulus and Poisson's ratio of the substrate, Y' and σ' are the Young's modulus and Poisson's ratio of the coating (here $\sigma' = 0.31$ [53]). ϕ_{\parallel} and ϕ_{\perp} are the mechanical loss values for the coating for strains parallel and perpendicular to the coating surface, d is the coating thickness and w_0 is the laser beam radius. In Fig. 6, the linear spectral density of the Brownian thermal noise arising from a multilayer GaP/AlGaP film is shown for 120 K and 20 K, as an indication of temperatures at which a future cryogenic detector may operate [1–3]. For comparison, the Brownian noise of an Advanced LIGO ETM on a silicon substrate, with the thicknesses adjusted for operation at 1550 nm, is plotted for 295 K, 120 K and 20 K.

The linear spectral density of the coating thermal noise is proportional to the temperature of the coating; therefore, cooling should provide a reduction in the thermal noise. However, it is also dependent on the mechanical loss of the

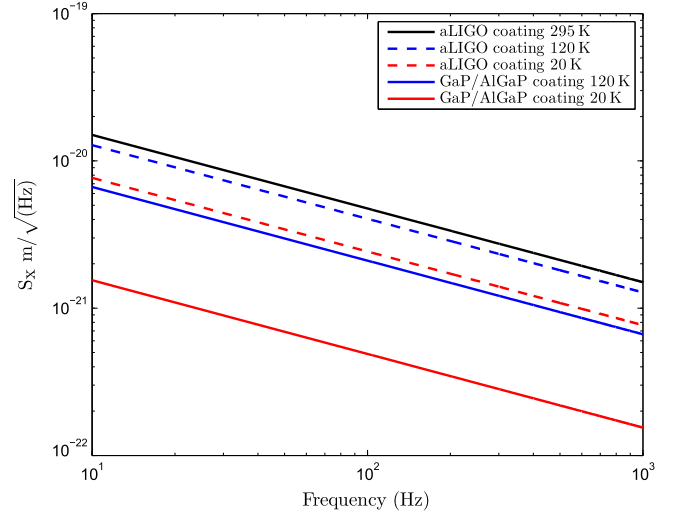


FIG. 6. Brownian thermal noise for an Advanced LIGO coating, optimised for 1550 nm, at 295 K (black), 120 K (dashed blue) and at 20 K (dashed red) and for a GaP/AlGaP coating at 120 K (blue) and at 20 K (red).

constituent coating materials, and sharp loss peaks have been observed at low temperatures in single layers of silica [57], titania-doped tantala [58] and in multilayer doped $\text{Ta}_2\text{O}_5/\text{SiO}_2$ films [59]. Consequently, as shown in Fig. 6, there is only a 40% improvement in the thermal noise of a similarly cooled Advanced LIGO coating. The low temperature loss peak observed in GaP is located at 50–70 K, and lies away from the 20 K and 120 K temperatures of interest for operation of future gravitational wave detectors. Despite the increase in the required total thickness of coating, the levels of Brownian thermal noise improve over an Advanced LIGO coating by almost 50% at 120 K, and by 80% at 20 K.

VII. CONCLUSION

In the gravitational wave detection era, there is a strong focus to improve the sensitivities of detectors like those used in Advanced LIGO. Thermal noise associated with mirror coatings is the most significant limit to the operating bandwidth sensitivity of the current generation of gravitational wave detectors. Epitaxially grown single-crystal coatings show considerable promise as alternatives to the ion-beam sputtered amorphous mirror coatings typically used in these detectors.

The mechanical loss of a $1 \mu\text{m}$ thick GaP coating, which incorporates a buffer layer necessary for the growth of high quality multilayer MBE GaP/AlGaP coatings on silicon, has been investigated over a broad range of frequencies and temperatures. At 295 K the upper limit of the loss of GaP film investigated here was higher than the loss reported in epitaxially grown GaP microdisks and is likely to be a

result of a defect driven process associated with the epitaxial growth on silicon.

For a reduced temperature of 120 K the loss of GaP improves to a factor of 7 lower than tantalum. At 20 K the upper limit of the loss of GaP was determined to be $2.7 \pm 0.2 \times 10^{-5}$, which is comparable to the loss of a multilayer GaP/AlGaP stack and a factor of 40 less than an undoped tantalum film heat-treated to 600 °C. The loss of the 1 μm thick layer studied here may be limited by defects in the buffer region, and the loss of GaP layers higher up the stack in a multilayer coating may potentially be even lower than the losses presented here.

There is evidence of an Arrhenius loss mechanism at 50–70 K which was found to have an activation energy of (94.7 ± 7.0) meV and rate constant of $(6.7 \pm 0.3) \times 10^{-12}$ s. In contrast with observations of GaP/AlGaP crystalline coatings, there was no evidence of any damage to the GaP coating after multiple temperature cycles between room temperature and 10 K.

The results presented here demonstrate that GaP is likely to be a good high-index material but further studies of GaP/AlGaP are of interest in order to identify the limiting source of loss, the nature of defects and to study the effects of MBE growth parameters on the loss and optical properties.

ACKNOWLEDGMENTS

We are grateful for the financial support provided by SUPA, STFC (ST/L000946/1 “Investigations in Gravitational Radiation”), the NSF through Grant No. PHY-1068596 and the University of Glasgow. IWM is supported by a Royal Society Research Fellowship. We are also grateful to the International Max Planck Partnership for Measurement and Observation at the Quantum Limit for support. We would like to thank our colleagues in SUPA, the LSC, Virgo, and KAGRA Collaborations for their interest in this work. This article has LIGO Document No. LIGO-P1600313.

-
- [1] The ETScience Team Collaboration, ET Technical Document No. ET-0106A-10, 2011.
- [2] R. Adhikari *et al.*, LIGO III Blue Concept, LIGO Technical Document No. LIGO-G1200573, 2012.
- [3] S. Hild *et al.*, LIGO 3 Strawman Design, Team Red, LIGO Technical Document No. LIGO-T1200046, 2012.
- [4] K. Somiya, *Classical Quantum Gravity* **29**, 124007 (2012).
- [5] Y. Sakakibara, T. Akutsu, D. Chen *et al.*, *Classical Quantum Gravity* **31**, 224003 (2014).
- [6] P. R. Saulson, *Fundamentals of Interferometric Gravitational Wave Detectors* (World Scientific Publishers, Singapore, 1994), ISBN 978-981-02-1820-1.
- [7] B. P. Abbott, R. Abbott, T. D. Abbott, M. R. Abernathy, F. Acernese, K. Ackley, C. Adams, T. Adams, P. Addesso, R. X. Adhikari *et al.*, *Phys. Rev. Lett.* **116**, 061102 (2016).
- [8] B. P. Abbott, R. Abbott, T. D. Abbott, M. R. Abernathy, F. Acernese, K. Ackley, C. Adams, T. Adams, P. Addesso, R. X. Adhikari *et al.* (LIGO Scientific Collaboration and Virgo Collaboration), *Phys. Rev. Lett.* **116**, 241103 (2016).
- [9] B. P. Abbott and the LIGO Scientific Collaboration, *Rep. Prog. Phys.* **72**, 076901 (2009).
- [10] G. M. Harry and the LIGO Scientific Collaboration, *Classical Quantum Gravity* **27**, 084006 (2010).
- [11] H. Grote and the LIGO Scientific Collaboration, *Classical Quantum Gravity* **25**, 114043 (2008).
- [12] H. Lück, C. Affeldt, J. Degallaix *et al.*, *J. Phys. Conf. Ser.* **228**, 012012 (2010).
- [13] T. Accadia, F. Acernese, M. Alshourbagy *et al.*, *J. Instrum.* **7**, P03012 (2012).
- [14] Y. Levin, *Phys. Rev. D* **57**, 659 (1998).
- [15] N. Nakagawa, A. M. Gretarsson, E. K. Gustafson, and M. M. Fejer, *Phys. Rev. D* **65**, 102001 (2002).
- [16] G. Harry, A. Gretarsson, P. Saulson, S. Kittelberger *et al.*, *Classical Quantum Gravity* **19**, 897 (2002).
- [17] D. R. M. Crooks, P. Sneddon, G. Cagnoli, J. Hough *et al.*, *Classical Quantum Gravity* **19**, 883 (2002).
- [18] K. Numata, A. Kemery, and J. Camp, *Phys. Rev. Lett.* **93**, 250602 (2004).
- [19] S. A. Webster, M. Oxborrow, and P. Gill, *Opt. Lett.* **29**, 1497 (2004).
- [20] T. Kessler, C. Hagemann, C. Grebing, T. Legero, U. Sterr, F. Riehle, M. J. Martin, L. Chen, and J. Ye, *Nat. Photonics* **6**, 687 (2012).
- [21] R. J. Rafac, B. C. Young, J. A. Beall, W. M. Itano, D. J. Wineland, and J. C. Bergquist, *Phys. Rev. Lett.* **85**, 2462 (2000).
- [22] A. D. Ludlow, T. Zelevinsky, G. K. Campbell, S. Blatt *et al.*, *Science* **319**, 1805 (2008).
- [23] F. Schmidt-Kaler, S. Gulde, M. Riebe, T. Deuschle, A. Kreuter, G. Lancaster, C. Becher, J. Eschner, H. Häffner, and R. Blatt, *J. Phys. B* **36**, 623 (2003).
- [24] M. Punturo, M. Abernathy, F. Acernese *et al.*, *Classical Quantum Gravity* **27**, 084007 (2010).
- [25] M. Punturo, M. Abernathy, F. Acernese *et al.*, *Classical Quantum Gravity* **27**, 194002 (2010).
- [26] S. Hild, M. Abernathy, F. Acernese *et al.*, *Classical Quantum Gravity* **28**, 094013 (2011).
- [27] S. Hild, *Classical Quantum Gravity* **29**, 124006 (2012).
- [28] O. L. Anderson and H. E. Bommel, *J. Am. Ceram. Soc.* **38**, 125 (1955).
- [29] M. E. Fine, H. van Duyne, and N. T. Kenney, *J. Appl. Phys.* **25**, 402 (1954).
- [30] J. W. Marx and J. M. Sivertsen, *J. Appl. Phys.* **24**, 81 (1953).
- [31] H. J. McSkimin, *J. Appl. Phys.* **24**, 988 (1953).

- [32] D. McGuigan, C. Lam, R. Gram, A. Hoffman, D. Douglass, and H. Gutche, *J. Low Temp. Phys.* **30**, 621 (1978).
- [33] R. Nawrodt, A. Zimmer, T. Koettig *et al.*, *J. Phys. Conf. Ser.* **122**, 012008 (2008).
- [34] S. Rowan, R. L. Byer, M. M. Fejer, R. K. Route, G. Cagnoli, D. R. Crooks, J. Hough, P. H. Sneddon, and W. Winkler, *Proc. SPIE* **4856**, 292 (2003).
- [35] W. Winkler, K. Danzmann, A. Rüdiger, and R. Schilling, *Phys. Rev. A* **44**, 7022 (1991).
- [36] M. J. Keever and M. A. Green, *Appl. Phys. Lett.* **66**, 174 (1995).
- [37] R. Schnabel, M. Britzger, F. Brückner, O. Burmeister, K. Danzmann, J. Duck, T. Eberle, D. Friedrich, H. Luck, M. Mehmet, R. Nawrodt, S. Steinlechner, and B. Willke, *J. Phys. Conf. Ser.* **228**, 012029 (2010).
- [38] G. D. Cole, W. Zhang, M. J. Martin, J. Ye, and M. Aspelmeyer, *Nat. Photonics* **7**, 644 (2013).
- [39] S. Adachi, *J. Appl. Phys.* **58**, R1 (1985).
- [40] P. Becker, P. Scyfried, and H. Siegert, *Z. Phys. B* **48**, 17 (1982).
- [41] M. Levinstein, S. Rumyantsev, and M. Shur, *Handbook Series on Semiconductor Parameters* (World Scientific, London, 1999).
- [42] S. M. Sze and K. K. Ng, *Physics of Semiconductor Devices* 3rd ed. (Wiley-Blackwell, New Jersey, 2006).
- [43] A. V. Cumming, K. Craig, I. W. Martin, R. Bassiri, L. Cunningham, M. M. Fejer, J. S. Harris, K. Haughian, D. Heinert, B. Lantz, A. C. Lin, A. S. Markosyan, R. Nawrodt, R. Route, and S. Rowan, *Classical Quantum Gravity* **32**, 035002 (2015).
- [44] A. C. Lin, M. M. Fejer, and J. S. Harris, *J. Cryst. Growth* **363**, 258 (2013).
- [45] I. W. Martin, R. Bassiri, R. Nawrodt *et al.*, *Classical Quantum Gravity* **27**, 225020 (2010).
- [46] R. Flaminio, J. Franc, C. Michel, N. Morgado, L. Pinard, and B. Sassolas, *Classical Quantum Gravity* **27**, 084030 (2010).
- [47] R. Nawrodt, C. Schwarz, S. Kroker, I. W. Martin *et al.*, *Classical Quantum Gravity* **30**, 115008 (2013).
- [48] A. Lin, LIGO Document No. G1200611-v1, 2012.
- [49] B. S. Berry and W. C. Pritchett, *IBM J. Res. Dev.* **19**, 334 (1975).
- [50] C. Zener, *Phys. Rev.* **52**, 230 (1937).
- [51] C. Zener, *Phys. Rev.* **53**, 90 (1938).
- [52] Y. S. Touloukian and E. H. Buyco, *Thermo-Physical Properties of Matter* (Plenum, New York, 1970).
- [53] W. F. Boyle and R. J. Sladek, *Phys. Rev. B* **11**, 2933 (1975).
- [54] Infrared Laboratories Inc, Tucson, Arizona, USA.
- [55] M. Mitchell, A. C. Hryciw, and P. E. Barclay, *Appl. Phys. Lett.* **104**, 141104 (2014).
- [56] A. Nowick and B. Berry, *Anelastic Relaxation in Crystalline Solids* (Academic Press, New York, 1972).
- [57] I. W. Martin, R. Nawrodt, K. Craig *et al.*, *Classical Quantum Gravity* **31**, 035019 (2014).
- [58] I. W. Martin, E. Chalkley, R. Nawrodt *et al.*, *Classical Quantum Gravity* **26**, 155012 (2009).
- [59] M. Granata, K. Craig *et al.*, *Opt. Lett.* **38**, 5268 (2013).